

Remarks on the quasinormal modes of Taub-NUT-AdS₄

Georgios Kalamakis[‡] and Anastasios C. Petkou[§]

*Laboratory of Theoretical Physics
Aristotle University of Thessaloniki
54124 Thessaloniki, Greece*

March 28, 2025

Abstract

We present results for the numerical evaluation of scalar quasinormal modes in Taub-NUT-AdS₄ spacetimes. To achieve this we consider angular modes that correspond to non-unitary highest weight $SU(2)$ representations since global regularity is not consistent with the presence of complex quasinormal modes. We show that for any non-zero value of the NUT charge n there exists a region in the complex plane that contains only stable quasinormal modes. The radius of this region increases with the horizon distance and decreases with n towards a constant value for infinite n . We also find analytic and numerical evidence for the existence of a critical NUT charge n_{cr} beyond which the lowest lying stable quasinormal modes become overdamped. Our results draw an intricate picture for the holographic fluid of Taub-NUT-AdS₄.

1 Introduction

The duality between asymptotically Anti-de Sitter spacetimes and relativistic hydrodynamical systems (see [1] for a review and references) is one of the most remarkable spinoffs of AdS/CFT holography and has generated among others an enormous interest in calculations of quasinormal modes (QNMs) for a wealth of black hole perturbations. Classical reviews on the subject include [2, 3].

Typically, the QNMs of asymptotically Anti-de Sitter black holes correspond to poles of the retarded Green's function of the dual holographic fluid system, and hence they are relevant to its dissipative properties. In this context, four-dimensional asymptotically AdS black holes are particularly interesting as they give rise to dissipative strongly coupled systems in 2+1 dimensions

[‡]georkal@hotmail.gr

[§]petkou@physics.auth.gr

which might be experimentally probed [4]. The seminal works on the QNMs of four-dimensional Schwarzschild AdS black holes [5–8] were followed by many studies of rotating [9, 10] and charged [11–14] asymptotically AdS black holes. Less explored are cases with nontrivial topology, of which the prime example is the Taub-NUT Anti-de Sitter (TNAdS) spacetime. The first effort towards the calculation of QNMs in TNAdS₄ was done in [15] and it was followed by the works [16, 17].

The main complication with the holographic interpretation of TNAdS₄ spacetimes arises due to the presence of the Misner string¹ [20–22]. At the level of perturbations around the background geometry the issue arises when one tries to solve the angular equation. For scalar perturbations this equation coincides with the equation that gives rise to the monopole harmonics [23] or equivalently the spin-weighted spherical harmonics [24, 25] and its regular solutions require the quantization of QNMs in units of the NUT charge [15]. This is equivalent to removing the Misner string at the expense of making periodic the time coordinate. Nevertheless, it was also argued in [15] that one might try to relax the regularity condition for the solutions of the angular equation which would be equivalent to allowing for a physical Misner string in the bulk. Such an approach would correspond to the presence of a vortex in the boundary fluid, having anyonic properties. For a recent discussion of the angular equation in Taub NUT spacetimes see [26].

In this note, following [15], we elaborate on the numerical evaluation of the QNMs of TNAdS₄ assuming the presence of a physical Misner string. In this case we cannot use regularity arguments to fix the eigenvalues of the angular equation, since the former condition is incompatible with the presence of complex QNMs. This should be contrasted with similar calculations of the angular modes in rotating black holes in [9, 10]. In the TNAdS₄ case, using the $SU(2)$ symmetry of the boundary metric as a guiding principle, we classify the angular modes into $SU(2)$ representations. These are, however, non-unitary and generically multivalued which would imply an anyonic behaviour of the holographic fluid parametrised by an arbitrary real parameter \mathcal{N} . We believe that the above properties of the angular modes are necessary for a possible holographic interpretation of TNAdS₄ spacetime as a dissipative fluid. In fact, one might compare the non-unitarity property of the $SU(2)$ representations with the corresponding property of the angular modes in rotating spacetimes, such as the Kerr-AdS₄, where the presence of complex QNMs is tied to complex eigenvalues of the angular equation [27] and appears to be closely connected with the chaotic properties of the holographic boundary fluid [28, 29].

We then show that for any non-zero value of the NUT charge n there exists a region in the complex plane that contains only stable quasinormal modes. The size of this *stable QNM region* is proportional to the horizon distance r_+ , hence larger TNAdS₄ black holes are more stable. When n increases the size of the stable QNM region decreases as $1/n$, but we find that it never shrinks to zero and tends to a constant value for infinite n . The behaviour of the quasinormal modes inside the stable QNM region depends crucially on n . For $n \ll 1$ the modes approach continuously the corresponding quasinormal modes of the Schwarzschild AdS₄ black hole. However, we observe

¹Recent works that propose a "rehabilitation" of TNAdS spacetimes include [18, 19].

that there exists a critical value for the NUT charge n_{cr} above which the real part of the lowest quasinormal mode falls abruptly to a near zero value and approaches zero for $n \gg n_{cr}$. The imaginary part of the lowest lying QNM also decreases abruptly as n approaches n_{cr} from above, but remains well above zero and moreover it starts increasing for $n > n_{cr}$. A similar behaviour is observed for the higher overtones. This picture does not seem to be affected by the anyonic parameter \mathcal{N} . Remarkably, the above critical value n_{cr} of the NUT charge seems to be rather insensitive to the horizon radius r_+ . We are then able to present a quantitative analytic argument what this is the case. Our results show that insisting on the presence of a physical Misner string leads to an intricate holographic fluid for TNAdS₄ whose salient property is the existence of a critical n_{cr} which separates a propagating from an overdamped phase. The alternative holographic interpretation would be that a superfluid with quantized vortices as we suggest. In Section 2 we setup the calculation by briefly reviewing the results of [15]. To calibrate our results we also review the well-known results for the QNMs of Schwarzschild AdS₄. In Section 3 we present the numerical methods of our calculations. In Section 4 we present and discuss our results.

2 Scalar fluctuations in Schwarzschild AdS₄ and Taub-NUT AdS₄ geometries.

The Lorentzian Schwarzschild and Taub-NUT AdS₄ metrics with spherical horizons can be collectively presented as²

$$ds^2 = g_{AB}dx^A dx^B = \frac{dr^2}{V(r, n)} + G(r, n) [d\theta^2 + \sin^2 \theta d\phi^2] - V(r, n)[dt + b(\theta, n)d\phi]^2 \quad (1)$$

with

$$V(r, n) = \frac{1}{r^2 + n^2} \left[r^2 - n^2 - 2Mr + \frac{1}{L^2}(r^4 + 6n^2 r^2 - 3n^4) \right], \quad (2)$$

$$G(r, n) = r^2 + n^2, \quad b(n, \theta) = 2n(1 - \cos \theta). \quad (3)$$

L is the AdS radius, $M > 0$ is the mass parameter and n is the NUT charge which is taken to be a real number. Schwarzschild SAdS₄ (SAdS₄) arises as a smooth limit of (1) for $n = 0$.

For generic values of $M > 0$ and n the above metric has an outer horizon at r_+ with the topology of S^2 . Its position is determined by $V(r_+, n) = 0$ as

$$r_+[r_+^3 + (6n^2 + L^2)r_+ - 2ML^2] = 3n^4 + n^2 L^2. \quad (4)$$

AdS/CFT proposes that the vacuum spacetimes (1) correspond to hydrodynamic systems living in their asymptotic timelike boundaries having a conserved, symmetric and traceless energy

²Throughout the paper we use $x^{(A,B)} = (r, t, \theta, \phi)$ and $x^{(\mu,\nu)} = (t, \theta, \phi)$.

momentum tensor whose expectation value in the fluid state is given as [30, 31]

$$T_{\mu\nu} = p[3u_\mu u_\nu + g_{\mu\nu}], \quad p = \frac{M}{8\pi G_4 L^2}, \quad \mu, \nu = 0, 1, 2, \quad (5)$$

$$\nabla^\mu T_{\mu\nu} = g^{\mu\nu} T_{\mu\nu} = 0, \quad T_{\mu\nu} = T_{\nu\mu}. \quad (6)$$

with G_4 the four-dimensional Newton's constant. The velocity u_μ of the boundary fluid's flow is a geodesic, shearless and expansionless congruence of the boundary metric

$$ds_{bdy}^2 = g_{\mu\nu} dx^\mu dx^\nu = -[dt + 2n(1 - \cos\theta)d\phi]^2 + L^2 d\Omega_2^2. \quad (7)$$

Due to the presence of the NUT parameter n the flow has nonzero vorticity³

$$u^\mu = (1, 0, 0), \quad u_\mu = (-1, 0, -2n(1 - \cos\theta)), \quad (8)$$

$$u^\nu \nabla_\nu u_\mu = \nabla_\mu u^\mu = \sigma_{\mu\nu} = 0, \quad (9)$$

$$\omega_{\mu\nu}^{TN} = \begin{pmatrix} 0 & 0 & 0 \\ 0 & 0 & -n \sin\theta \\ 0 & n \sin\theta & 0 \end{pmatrix}. \quad (10)$$

Having at hand the vorticity one can calculate its flux through a bounded surface i.e. the circulation. For inviscid and barotropic fluids the circulation along any closed path is constant and hence one would expect from Stoke's theorem that the vorticity flux through a closed surface is zero. This can be verified for example in the case of the rotating boundary fluid of the Kerr-AdS₄ metric [15]. However, in the TNAdS₄ case the flow velocity (8) is singular⁴ at $\theta = \pi$ and one needs to invoke Stoke's theorem for non simply connected domains. The result is that the total circulation, or equivalently the vorticity flow over the S^2 boundary surface, does not vanish and it is given by

$$\mathcal{C}_{tot}^{TN} = 2 \oint\!\!\!\oint_S dS^{\mu\nu} \omega_{\mu\nu}^{TN} = -2n \int_0^{2\pi} d\phi \int_0^\pi d\theta \sin\theta = -8\pi n. \quad (11)$$

Finally, since the metric (7) is not conformally flat, it gives rise to a non-zero Cotton tensor that has the form of a perfect conformal fluid [32].

$$C_{\mu\nu} = \frac{n}{L^4} \left(1 + \frac{4n^2}{L^2} \right) [3u_\mu u_\nu + g_{\mu\nu}], \quad \nabla^\mu C_{\mu\nu} = g^{\mu\nu} C_{\mu\nu} = 0. \quad (12)$$

3 The quasinormal modes of TNAdS₄

The holographic interpretation of TNAdS₄ is, to our knowledge, still an open issue. While $T_{\mu\nu}$ gives the expectation value of the energy momentum tensor in a thermal state of the boundary

³Recall the definitions of acceleration $\alpha_\mu = u^\nu \nabla_\nu u_\mu$, expansion $\Theta = \nabla_\mu u^\mu$, shear $\sigma_{\mu\nu} = h_\mu^\sigma h_\nu^\rho (\nabla_\sigma u_\rho + \nabla_\rho u_\sigma)/2 - h_{\mu\nu} h^{\sigma\rho} (\nabla_\sigma u_\rho)/2$ and vorticity $\omega_{\mu\nu} = h_\mu^\sigma h_\nu^\rho (\nabla_\sigma u_\rho - \nabla_\rho u_\sigma)/2$, where $h_{\mu\nu} = g_{\mu\nu} + u_\mu u_\nu$. One might interpret u as a gauge field, ω as the corresponding field strength, and the circulation \mathcal{C} (eq. (11)) as a charge.

⁴This can be seen as $\hat{u} \xrightarrow{\theta \rightarrow 0} -dt + \theta n L \hat{e}^\phi + O(\theta^3)$, $\hat{u} \xrightarrow{\theta \rightarrow \pi} -dt + \frac{nL}{\pi - \theta} \hat{e}^\phi + O(\pi - \theta)$, $\hat{e}^\phi = \sin\theta d\phi$.

system, the Cotton tensor $C_{\mu\nu}$ arises as a property of the boundary metric (7) which in the context of AdS/CFT is interpreted as an external source of the boundary effective action. We therefore believe that the natural interpretation of $C_{\mu\nu}$ is that of a source for an operator in the boundary system, which is probably nonlocal and similar to the monopole operator in electromagnetism. Hence, the holographic boundary fluid appears to be more intricate than the rotating fluid of e.g. Kerr-AdS₄.

Nevertheless, whatever the holographic interpretation of the NUT charge n is, one can easily verify that the TNAdS₄ metric becomes Schwarzschild AdS₄ in the limit $n \rightarrow 0$ and that the limit is geometrically smooth. Moreover, there does not appear to exist an upper bound on n similar to the upper bound of the rotation parameter in Kerr-AdS₄, nor is there a useful extremal limit such as in the case of charged AdS black holes. We hope to shed partial light on these issues by studying the scalar quasinormal modes of the Taub-NUT AdS₄ metric. For simplicity we consider a minimally coupled scalar field Φ whose equation of motion on the fixed metric (1) is

$$\frac{1}{\sqrt{-g}}\partial_A[\sqrt{-g}g^{AB}\partial_B\Phi] = 0. \quad (13)$$

This equation is separable and assuming $\Phi(t, r, \theta, \phi) = e^{-i\omega t}R(r)Y(\theta, \phi)$ one obtains the set of equations

$$\left\{ \frac{d}{dr}[G(r, n)V(r, n)\frac{d}{dr}] + \omega^2\frac{G(r, n)}{V(r, n)} + 4n^2\omega^2 - C \right\} R(r) = 0, \quad (14a)$$

$$\{\mathbf{L}^2 - C\} Y(\theta, \phi) = 0, \quad (14b)$$

where

$$\mathbf{L}^2 = -\frac{1}{\sin^2\theta} \left[\sin\theta\frac{\partial}{\partial\theta} \left(\sin\theta\frac{\partial}{\partial\theta} \right) + [\partial_\phi + i2n\omega(1 - \cos\theta)]^2 \right] + 4n^2\omega^2. \quad (15)$$

The separation constant C corresponds to the quadratic Casimir of an $SU(2)$ representation, see [15] and the discussion below.

From the outset equations (14a) and (14b) look very similar to the set of Teukolsky equations for Kerr perturbations e.g. [9]. However, contrary to these cases TNAdS₄ geometry possesses a richer geometrical structure which should play a role in the analysis of the fluctuation equations above. Explicitly, the boundary metric (7) has an $SU(2) \times \mathbb{R}$ isometry generated by the vector fields⁵

$$\xi_1 = -\sin\phi\cot\theta\partial_\phi + \cos\phi\partial_\theta - 2n\sin\phi\frac{1 - \cos\theta}{\sin\theta}\partial_t, \quad (16)$$

$$\xi_2 = \cos\phi\cot\theta\partial_\phi + \sin\phi\partial_\theta + 2n\cos\phi\frac{1 - \cos\theta}{\sin\theta}\partial_t, \quad (17)$$

$$\xi_3 = \partial_\phi - 2n\partial_t, \quad \mathbf{e} = \partial_t \quad (18)$$

with

$$[\xi_i, \xi_j] = -\epsilon_{ijk}\xi_k \quad [\xi_i, \mathbf{e}] = 0 \quad i, j, k = 1, 2, 3. \quad (19)$$

⁵The interested reader is asked to look in [15] for more details.

We conclude that the angular eigenfunctions $Y(\theta, \phi)$ can be classified according to representations of $SU(2)$, in contrast to the Kerr-AdS₄ case where there is no such requirement. Notice that when $n = 0$ the angular equation (14b) becomes the equation that gives the usual spherical harmonics which are the unitary finite dimensional representations of $SU(2)$. To proceed we can define the complex generators as

$$\mathbf{L}_3 = -i\xi_3 = -i(\partial_\phi - 2n\partial_t), \quad \mathbf{L}_\pm = \pm\xi_1 + i\xi_2, \quad (20)$$

which satisfy

$$[\mathbf{L}_+, \mathbf{L}_-] = 2\mathbf{L}_3 \quad [\mathbf{L}_3, \mathbf{L}_\pm] = \pm\mathbf{L}_\pm. \quad (21)$$

It is then straightforward to verify that the quadratic $SU(2)$ Casimir is given by

$$\mathbf{L}^2 = -\sum_i \xi_i^2. \quad (22)$$

It is convenient to write the eigenvalue of the quadratic Casimir as $C = q(q + 1)$ and look for solutions of the angular equation on which \mathbf{L}_\pm act as raising/lowering operators. Such solutions are the eigenfunctions of the "magnetic" operator $\mathbf{L}_3 = -i\xi_3$. Namely we ask that

$$\mathbf{L}^2 Y(\theta, \phi) = C Y(\theta, \phi), \quad \mathbf{L}_3 Y(\theta, \phi) = m Y(\theta, \phi). \quad (23)$$

Due to the form of \mathbf{L}_3 , to satisfy the second of (23) we need to have

$$Y(\theta, \phi) \equiv Y_{q,m,\Omega}(\theta, \phi) = Y_{q,m,\Omega}(\theta) e^{i\mathcal{N}\phi}, \quad (24)$$

where we have set $\mathcal{N} = m - \Omega$ and $\Omega = 2n\omega$. This form of the angular eigenfunctions is a salient feature of the TNAdS₄ fluctuations if we insist that they should fall into $SU(2)$ representations. Namely, the azimuthal ϕ -dependence of the fluctuations depends on the mode frequency ω . Given the form of (24) eq. (14b) becomes

$$\left\{ \frac{1}{\sin\theta} \frac{d}{d\theta} \left[\sin\theta \frac{d}{d\theta} \right] - \frac{(m - \Omega \cos\theta)^2}{\sin^2\theta} - \Omega^2 + q(q + 1) \right\} Y_{q,m,\Omega}(\theta) = 0. \quad (25)$$

A few remarks are in order here. Eq. (25) coincides with the equation satisfied by the *spin-weighted spheroidal harmonics* [33] if we were to set $\Omega \equiv s = 0, \pm 1, \pm 2, \dots$. This quantization condition on Ω would give us a handle on the functions $Y(\theta, \phi)$ which can then be identified with the everywhere regular spin-weighted spherical harmonics and can be constructed from the usual spherical harmonics by repeated applications of spin-raising operators [34]. This approach is equivalent to the quantum mechanical description of a particle with charge $e \equiv \omega$ in a magnetic monopole background, with $g \equiv -2n$ the monopole charge [35].

However, the intricacy of our problem lies in the fact that $\Omega = 2n\omega$ is not necessarily quantized. In fact, it is independently determined by the radial equation (14a) which will generically give

complex values for ω if we impose the usual infalling boundary condition on r_+ . We are therefore forced to conclude that the regularity of the angular modes is incompatible with the presence of complex quasinormal modes. For that reason we developed in [15] an approach to solve the angular equation (25) that allows for complex quasinormal modes Ω at the expense of the regularity of the angular eigenfunctions. Let us briefly review this here. Introducing the coordinate $u = \sin^2(\theta/2)$ (25) becomes

$$\left\{ \frac{d}{du} \left[u(1-u) \frac{d}{du} \right] + \left[q(q+1) - \Omega^2 - \frac{(\mathcal{N} + 2u\Omega)^2}{4u(1-u)} \right] \right\} Y_{q,m,\Omega}(u) = 0, \quad (26)$$

whose solutions are hypergeometric functions of the form

$$Y_{q,m,\Omega}(u) = u^{a/2} (1-u)^{b/2} {}_2F_1(1+q + \frac{a+b}{2}, -q + \frac{a+b}{2}; 1+a; u). \quad (27)$$

The parameters a, b take four possible values $a = \pm\mathcal{N}$, $b = \pm(2m - \mathcal{N})$, however the resulting four hypergeometric functions are not all independent and it suffices to consider

$$Y_{q,m,\Omega}^\pm(u) = u^{\pm\mathcal{N}/2} (1-u)^{\pm(2m-\mathcal{N})/2} {}_2F_1(1+q \pm m, -q \pm m; 1 \pm \mathcal{N}; u). \quad (28)$$

Overall the solutions to the scalar wave equation take the form

$$\Phi_{q,m,\Omega}^\pm(t, r, u, \phi) = R_{q,\Omega}(r) \Psi_{q,m,\Omega}^\pm(t, u, \phi), \quad (29)$$

$$\Psi_{q,m,\Omega}^\pm(t, u, \phi) = e^{-i\omega t} Y_{q,m,\Omega}^\pm(u, \phi) = e^{-i\omega t} e^{i\mathcal{N}\phi} Y_{q,m,\Omega}^\pm(u), \quad (30)$$

and satisfy

$$ie(\Psi_{q,m,\Omega}^\pm(t, u, \phi)) = \omega \Psi_{q,m,\Omega}^\pm(t, u, \phi), \quad (31)$$

$$\mathbf{L}_3(\Psi_{q,m,\Omega}^\pm(t, u, \phi)) = m \Psi_{q,m,\Omega}^\pm(t, u, \phi), \quad (32)$$

$$\mathbf{L}^2(\Psi_{q,m,\Omega}^\pm(t, u, \phi)) = q(q+1) \Psi_{q,m,\Omega}^\pm(t, u, \phi). \quad (33)$$

The action of the raising/lowering operators \mathbf{L}_\pm on the $SU(2)$ modules can be found using their explicit forms

$$\mathbf{L}_\pm = \frac{ie^{\pm i\phi}}{\sqrt{u(1-u)}} \left[\mp iu(1-u)\partial_u + \frac{1-2u}{2}\partial_\phi + 2nu\partial_t \right], \quad (34)$$

as

$$\mathbf{L}_-(\Psi_{q,m,\Omega}^+(t, u, \phi)) = -\mathcal{N}\Psi_{q,m-1,\Omega}^+(t, u, \phi), \quad (35)$$

$$\mathbf{L}_+(\Psi_{q,m,\Omega}^+(t, u, \phi)) = \frac{(1+q+m)(m-q)}{1+\mathcal{N}} \Psi_{q,m+1,\Omega}^+(t, u, \phi), \quad (36)$$

$$\mathbf{L}_-(\Psi_{q,m,\Omega}^-(t, u, \phi)) = \frac{(1+q-m)(m+q)}{1-\mathcal{N}} \Psi_{q,m-1,\Omega}^-(t, u, \phi), \quad (37)$$

$$\mathbf{L}_+(\Psi_{q,m,\Omega}^-(t, u, \phi)) = -\mathcal{N}\Psi_{q,m+1,\Omega}^-(t, u, \phi). \quad (38)$$

Eqs (35)-(38) are just the known relations satisfied by $SU(2)$ representations. The difference wrt to the standard quantum mechanical case are that i) the \mathbf{L}_3 eigenvalue \mathcal{N} is not necessarily integer, and ii) the $SU(2)$ modules are non necessarily finite dimensional.

To proceed we make two further assumptions. Firstly we assume that $\mathcal{N} = m - \Omega \in \mathbb{R}$. The physical implication of our assumption is that the angular modes are *anyonic* and we want to attribute such a property to the presence of physical Misner string. Secondly, since the solutions of (25) span an $SU(2)$ representation space, we can arrange them in highest/lowest weight modules. To do that notice that if $Y_{q,m,\Omega}(u, \phi)$ is a solution of eq. (14b) corresponding to the quasinormal mode ω , then $Y_{q,m,\Omega}^*(u, \phi) \equiv \tilde{Y}_{\bar{q},\bar{m},\bar{\Omega}}(u, \phi)$ solves the same equation for values of the parameters $(q^*, -m^*, -\Omega^*) \equiv (\bar{q}, \bar{m}, \bar{\Omega})$, and $\bar{\mathcal{N}} = -\mathcal{N}$. The two complex conjugate solutions are

$$Y_{q,m,\Omega}(u, \phi) = e^{i\mathcal{N}\phi} u^{\mathcal{N}/2} (1-u)^{(2m-\mathcal{N})/2} {}_2F_1(1+q+m, -q+m, 1+m-\Omega; u), \quad (39)$$

$$\tilde{Y}_{\bar{q},\bar{m},\bar{\Omega}}(u, \phi) = e^{i\bar{\mathcal{N}}\phi} u^{-\bar{\mathcal{N}}/2} (1-u)^{-(2\bar{m}-\bar{\mathcal{N}})/2} {}_2F_1(1+\bar{q}-\bar{m}, -\bar{q}-\bar{m}, 1-\bar{m}+\bar{\Omega}; u). \quad (40)$$

We then obtain

$$\mathbf{L}_- \left(e^{-i\bar{\omega}t} \tilde{Y}_{\bar{q},\bar{m},\bar{\Omega}}(u, \phi) \right) = \frac{(1+\bar{q}-\bar{m})(-\bar{q}-\bar{m})}{1-\bar{m}+\bar{\Omega}} e^{-i\bar{\omega}t} \tilde{Y}_{\bar{q},\bar{m}-1,\bar{\Omega}}(u, \phi), \quad (41)$$

and

$$\mathbf{L}_+ \left(e^{-i\omega t} Y_{q,m,\Omega}(u, \phi) \right) = \frac{(1+q+m)(m-q)}{1+m-\Omega} e^{-i\omega t} Y_{q,m+1,\Omega}(u, \phi). \quad (42)$$

Therefore we can associate $Y_{q,q,\Omega}(u, \phi)$ to a highest weight state $\Psi_{q,q,\Omega}(t, u, \phi)$ that is annihilated by the raising operator as $\mathbf{L}_+ \Psi_{q,q,\Omega}(t, u, \phi) = 0$, while $\tilde{Y}_{\bar{q},-\bar{q},\bar{\Omega}}(u, \phi)$ to a corresponding lowest weight state with $\mathbf{L}_- \tilde{\Psi}_{\bar{q},-\bar{q},\bar{\Omega}}(t, u, \phi) = 0$. The highest/lowest weight modules are infinite dimensional, hence they form non-unitary representations of $SU(2)$. To every highest/lowest weight module correspond the quasinormal modes $\omega / -\omega^*$ respectively. Notice that the finite-dimensional degeneracy of the quasinormal modes in the SAdS₄ case has become infinite-dimensional. This is reminiscent of Landau modes (see a related discussion in [36]).

In our discussion for the solutions of angular equation we were agnostic regarding the possible values of the parameters q, m and Ω . For example, they can take complex values which we denote as

$$q = q_1 + iq_2, \quad m = m_1 + im_1, \quad \Omega = \Omega_1 + i\Omega_2. \quad (43)$$

Consider then a highest weight state with $q = m$ and use the condition that $m - \Omega = \mathcal{N} \in \mathbb{R}$. These lead to

$$q = q_1 + iq_2 = m_1 + im_2 = \Omega_1 + \mathcal{N} + i\Omega_2 = \Omega + \mathcal{N}. \quad (44)$$

This determines the separation constant C of the angular equation 14b) as⁶

$$C = (\Omega + \mathcal{N} + 1)(\Omega + \mathcal{N}). \quad (45)$$

⁶If we further require this to be real we find [15] $C = -\frac{1}{4} - \Omega_2^2$, $\mathcal{N} = -\frac{1}{2} - \Omega_1$.

4 Numerical evaluation of the quasinormal modes

Our deliberations above did not fully address the issue with the angular equation, however they provide a working path towards the numerical calculation of the quasinormal modes. Our strategy is to substitute (45) for C in the radial equation (14a). This way \mathcal{N} remains as an arbitrary real parameter. In the following we will consider the case $\mathcal{N} = 0$ and we will see that the dependence of our results on $\mathcal{N} \in [-2, 2]$ is rather weak.

4.1 Qualitative features

The treatment of the radial equation proceeds in a standard manner. We start by setting

$$R(r) = \frac{1}{\sqrt{G(r, n)}} Z(r), \quad (46)$$

and we obtain from (14a)

$$V(r, n)Z''(r) + V'(r, n)Z'(r) + \left[\omega^2 \frac{h^2(r, n)}{V(r, n)} - U(r, n) \right] Z(r) = 0, \quad (47)$$

with

$$U(r, n) = \frac{rV'(r, n) + C}{G(r, n)} + \frac{n^2V(r, n)}{G^2(r, n)}, \quad h^2(r, n) = 1 + \frac{4n^2V(r, n)}{G(r, n)}, \quad (48)$$

where the prime denotes differentiation with respect to r . We can also write $V(r, n)$ in terms of the horizon distance r_+ by eliminating M in (4) as

$$V(r, n) = \frac{1}{r^2 + n^2} \left(r^2 - n^2 + \frac{1}{L^2} (r^4 + 6n^2r^2 - 3n^4) - \frac{r}{L^2r_+} (r_+^4 + L^2r_+^2 + 6n^2r_+^2 - L^2n^2 - 3n^4) \right). \quad (49)$$

$V(r, n)$ is positive for all $r \in [r_+, \infty)$ and it develops a local maximum and a local minimum when n is large enough compared to r_+ [15]. The temperature T is defined in the standard way as (we set $L = 1$ onwards)

$$T = \frac{V'(r_+, n)}{4\pi} = \frac{1 + 3r_+^2 + 3n^2}{4\pi r_+}, \quad (50)$$

and for fixed r_+ it grows as $T \sim n^2$.

Next we impose the infalling boundary conditions at the horizon writing

$$Z(r) = e^{-i\omega r_*} \Psi(r). \quad (51)$$

The tortoise coordinate r_* is defined as⁷

$$\frac{dr_*}{dr} = \frac{h(r, n)}{V(r, n)} \Rightarrow r_* \sim \frac{1}{4\pi T r_+} \ln(r - r_+) + \dots, \quad (52)$$

⁷In the tortoise coordinate the horizon is at $r_* \rightarrow -\infty$ and the boundary at $r_* \rightarrow \infty$.

with the dots denoting higher powers in $(r - r_+)$. This brings (47) to the form

$$V(r, n)\Psi''(r) + [V'(r, n) - 2i\omega h(r, n)]\Psi'(r) - [i\omega h'(r, n) + U(r, n)]\Psi(r) = 0. \quad (53)$$

This form is useful in order to acquire a qualitative picture for the quasinormal modes. Multiplying (53) with $\Psi^*(r)$ and integrating from r_+ to infinity we obtain

$$\int_{r_+}^{\infty} (-V(r, n)|\Psi'(r)|^2 - 2i\omega h(r, n)\Psi^*(r)\Psi'(r) - [i\omega h'(r, n) + U(r, n)]|\Psi(r)|^2) dr = 0. \quad (54)$$

Taking the complex conjugate of the above and setting $C = (\Omega + 1)\Omega$ we get

$$\int_{r_+}^{\infty} [V(r, n)|\Psi'(r)|^2 + \mathcal{A}(r, n; \omega)|\Psi(r)|^2] dr = -\frac{|\omega|^2}{\text{Im}(\omega)}|\Psi(r_+)|^2. \quad (55)$$

with

$$\mathcal{A}(r, n; \omega) = \frac{rV'(r, n)}{G(r, n)} + \frac{n^2V(r, n)}{G^2(r, n)} - \frac{4n^2|\omega|^2}{G(r, n)}. \quad (56)$$

When $n = 0$ the integrand on the l.h.s. of (55) is positive, which shows that the quasinormal modes of SAdS₄ can only have negative imaginary part and hence they are stable. For $n \neq 0$ we note⁸ that

$$\lim_{r \rightarrow r_+} \mathcal{A}(r, n; \omega) = \frac{1}{r_+^2 + n^2} (1 + 3r_+^2 + 3n^2 - 4n^2|\omega|^2), \quad \lim_{r \rightarrow \infty} \mathcal{A}(r, n; \omega) = 2. \quad (57)$$

Therefore, if

$$|\omega|^2 \leq |\omega_*(r_+, n)|^2 = \frac{1 + 3r_+^2 + 3n^2}{4n^2}, \quad (58)$$

then $\mathcal{A}(r, n; \omega)$ is positive for $r \in [r_+, \infty)$ and hence the corresponding quasinormal modes are stable. The typical behaviour of $\mathcal{A}(r, n, ; \omega)$ is plotted for $r_+ = n = 1$ in Fig.1. This analysis shows

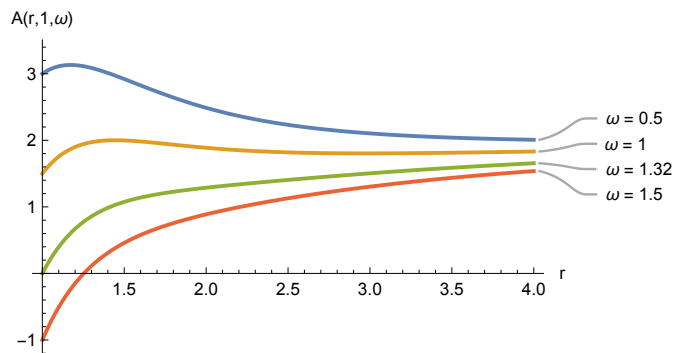


Figure 1: Typical plots of $A(r, 1; \omega)$ for $|\omega_*| = \frac{\sqrt{7}}{2} \approx 1.32$.

that for a given $n \neq 0$ there always exist a region in the complex plane of the quasinormal modes ω , which can be thought of as a circle centered at the origin, that contains only stable modes. The value $|\omega_*(r_+, n)|$ is clearly a lower bound for the radius of this *stable QNM region* and it grows

⁸ $\mathcal{A}(r, n; \omega)$ depends on n^2 .

linearly with r_+ for large r_+ . Hence large TNAdS₄ black holes have a larger stable QNM region. On the other hand $|\omega_*(r_+, n)|$ for fixed r_+ is proportional to $1/n$ therefore the stable QNM region shrinks as n increases. Interestingly though, this region never shrinks to a point as the limit $n \rightarrow \infty$ of (58) is finite and gives

$$\lim_{n \rightarrow \infty} |\omega_*(r_+, n)| = \frac{\sqrt{3}}{2}. \quad (59)$$

It would be nice to understand this limiting case further.

4.2 Setting up the numerical algorithm

We set up the numerical algorithm for the calculation of the QNMs using following the seminal work [5]. If we define

$$h(r, n)\psi(r) = \Psi(r), \quad (60)$$

the radial equation becomes

$$V(r, n)\psi''(r) + V_1(r, n)\psi'(r) + V_2(r, n)\psi(r) = 0, \quad (61)$$

where

$$V_1(r, n) = V'(r, n) - V(r, n)\frac{h'(r, n)}{h(r, n)} - 2i\omega h(r, n), \quad (62)$$

$$V_2(r, n) = \frac{3V(r, n)(h'(r, n))^2}{4h(r, n)^2} - \frac{V(r, n)h''(r, n)}{2h(r, n)} - \frac{V'(r, n)h'(r, n)}{2h(r, n)} - U(r, n). \quad (63)$$

We now ask that $\psi(r_+)$ is finite and as a final step we make the change of variables $z = r_+/r$ such that the horizon is at $z = 1$ and the boundary at $z = 0$. In the z variable the potential $V(r, n) \mapsto V(z, n)$ with

$$V(z, n) = \frac{\frac{r_+^4}{z^2} + (1 + 6n^2)r_+^2 - z[r_+^2(1 + r_+^2) - n^2(1 - 6r_+^2 + 3n^2)] - n^2(1 + 3n^2)z^2}{r_+^2 + n^2z^2}, \quad (64)$$

and the final form of the radial equation becomes

$$s(z)\psi''(z) + \frac{t(z)}{z-1}\psi'(z) - \frac{u(z)}{(z-1)^2}\psi(z) = 0, \quad (65)$$

where

$$\begin{aligned} s(z) &= V(z, n), & t(z) &= \frac{z-1}{z} \left[2V(z, n) + zV'(z, n) - zV(z, n)h_1(z, n) + \frac{2i\omega r_+}{z}h(z, n) \right], \\ u(z) &= (z-1)^2 \left[U(z, n) + \frac{z^4}{4}V(z, n) \left(-3h_1^2(z, n) + 2h(z, n)h_2(z, n) - \frac{4}{z}h_1(z, n) \right) \right. \\ &\quad \left. + \frac{z^4}{2}h_1(z, n)V'(z, n) \right], \end{aligned}$$

$$U(z, n) = \frac{Cz^2}{r_+^2 + n^2z^2} - \frac{z^3}{r_+^2 + n^2z^2}V'(z, n) + \frac{z^4n^2V(z, n)}{(r_+^2 + n^2z^2)^2},$$

and we have defined

$$h_1(z, n) = \frac{h'(z, n)}{h(z, n)}, \quad h_2(z, n) = \frac{h''(z, n)}{h^2(z, n)}. \quad (66)$$

One can check that for $n = 0$ the functions above coincide⁹ with the ones in [5]. Now the horizon $z = 1$ is a regular singular point of the differential equation (65) since the functions $s(z)$, $t(z)$ and $u(z)$ have regular expansions around it as

$$s(z) = \sum_{k=0}^{\infty} s_k(z-1)^k, \quad t(z) = \sum_{k=0}^{\infty} t_k(z-1)^k, \quad u(z) = \sum_{k=0}^{\infty} u_k(z-1)^k, \quad (67)$$

Therefore, near $z = 1$ we look for a series solution of the form

$$\psi(z) = (z-1)^a \sum_{k=0}^{\infty} \psi_k(\omega)(z-1)^k, \quad (68)$$

where the coefficients ψ_k are functions of ω and \mathcal{N} through the relation $C = C(\Omega, \mathcal{N})$ in (45).

From (65) using (68) we find the indicial equation at the horizon as

$$a(a-1)s_0 + at_0 - u_0 = 0, \quad (69)$$

where

$$s_0 = -\frac{4\pi T}{r_+}, \quad t_0 = -\frac{2}{r_+}(2\pi T - i\omega), \quad u_0 = 0, \quad (70)$$

and the temperature is defined in (50). The indicial equation is solved giving $a = 0$ or $a = i\omega/2\pi T$. The second solution would give the outgoing modes near the horizon, so we set $a = 0$ from now on.

Substituting (67) and (68) into (65) we get the following recursion relation for the coefficients $\psi_m(\omega)$

$$\psi_m(\omega) = \frac{1}{m(m-1)s_0 + mt_0} \sum_{k=0}^{m-1} \left[u_{m-k} - kt_{m-k} - k(k-1)s_{m-k} \right] \psi_k(\omega), \quad (71)$$

Finally, the quasinormal modes are the complex roots ω of the polynomial equation that enforces the Dirichlet boundary conditions at the boundary, namely

$$\psi(0) = \sum_{k=0}^{\infty} \psi_k(\omega)(-1)^k = 0. \quad (72)$$

4.3 Numerical results and critical NUT charge

Our numerical routines follow closely the standard ones¹⁰ and can be made available upon request. From the outset it is important to emphasise that below we present results for "half" of the quasinormal modes, namely those whose lowest mode has a positive real part. The other half can be

⁹When $n = 0$ we have to set $\Omega = 0$ and $\mathcal{N} = m \in \mathbb{Z}$.

¹⁰See for example <https://centra.tecnico.ulisboa.pt/network/grit/files/ringdown/>.

obtained by the transformation $\omega \rightarrow -\omega^*$ which is a symmetry of the equations as explained above. For clarity and numerical stability we focus on two regimes: a) "large" BHs with $r_+ \gg 1$ and b) "intermediate" BHs with $r_+ \sim 1$. A salient feature of the SAdS₄ QNMs is that the ratio ω/r_+ for the lowest QNM is constant for both large and intermediate BHs, and it is only slightly different for the two regimes. The proportionality constant depends on the angular momentum of the modes.

Firstly we focus on the lowest QNMs. We present in Tables 1 and 2 below the numerical results for the real part ω_R and for minus the imaginary part $-\omega_I$ of the lowest QNMs, as well and for its norm $|\omega|$, for typical values of r_+ in the large and intermediate regimes. We start our calculations for $n = 0$ to reproduce the results of [5] and then we increase n .

Table 1: The lowest QNMs in intermediate TNAdS₄ black holes

r_+	n	Re $[\omega]$	-Im $[\omega]$	$ \omega $
0.4	0.000	2.37	1.16	2.64
0.4	0.001	2.36	1.16	2.63
0.4	0.002	2.36	1.16	2.63
0.4	0.01	2.34	1.15	2.61
0.4	0.1	2.13	1.13	2.41
0.6	0.000	2.45	1.58	2.91
0.6	0.001	2.44	1.58	2.91
0.6	0.002	2.44	1.58	2.91
0.6	0.01	2.42	1.57	2.89
0.6	0.1	2.23	1.55	2.72

r_+	n	Re $[\omega]$	-Im $[\omega]$	$ \omega $
0.8	0.000	2.59	2.13	3.35
0.8	0.001	2.59	2.13	3.35
0.8	0.002	2.58	2.13	3.35
0.8	0.01	2.57	2.12	3.33
0.8	0.1	2.39	2.06	3.15
1.0	0.000	2.8	2.67	3.87
1.0	0.001	2.8	2.67	3.87
1.0	0.002	2.79	2.67	3.86
1.0	0.01	2.78	2.66	3.84
1.0	0.1	2.6	2.58	3.66

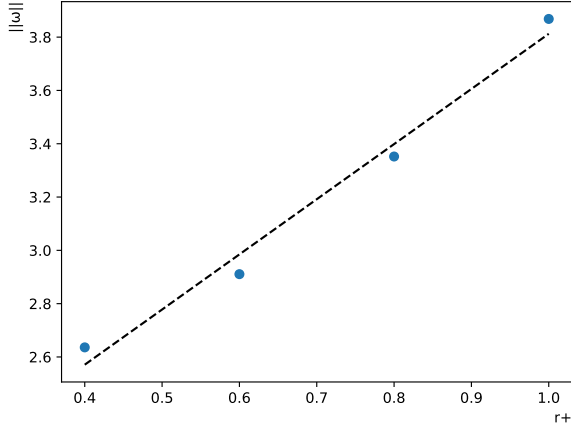
Table 2: The lowest QNMs in large TNAdS₄ black holes

r_+	n	Re $[\omega]$	-Im $[\omega]$	$ \omega $
5	0.000	9.47	13.33	16.35
5	0.001	9.47	13.32	16.35
5	0.002	9.47	13.32	16.34
5	0.010	9.45	13.31	16.32
5	0.100	9.27	13.16	16.09
10	0.000	18.61	26.64	32.5
10	0.001	18.6	26.64	32.49
10	0.002	18.6	26.64	32.49
10	0.01	18.59	26.62	32.47
10	0.1	18.41	26.47	32.24

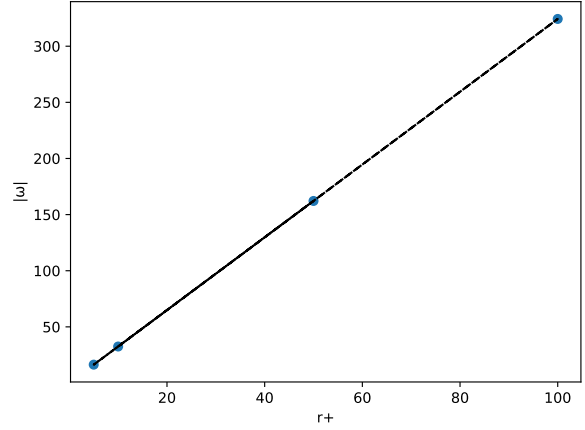
r_+	n	Re $[\omega]$	-Im $[\omega]$	$ \omega $
50	0.000	92.49	133.19	162.16
50	0.001	92.49	133.19	162.16
50	0.002	92.49	133.19	162.15
50	0.01	92.47	133.18	162.13
50	0.1	92.33	133.03	161.93
100	0.000	184.95	266.38	324.3
100	0.001	184.95	266.38	324.29
100	0.002	184.95	266.38	324.29
100	0.01	184.93	266.37	324.27
100	0.1	184.84	266.24	324.11

For small values of $n \in [0, 0.1]$, we notice that ω_R, ω_I and $|\omega|$ they all decrease but only slightly w.r.t the SAdS₄ values. In the large black hole regime the ratio $|\omega|/r_+$ stays approximately constant, while in the intermediate regime the relation exhibits a mild non-linearity. This can be seen in figures 2. The approximate formulae for the large and intermediate regime are

$$|\omega|_{intermediate} = 2.07r_+ + 1.74 \quad |\omega|_{large} = 3.24r_+. \quad (73)$$



(a) Intermediate horizon regime.

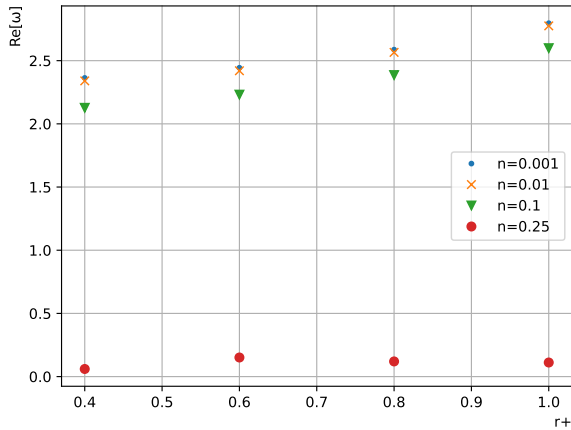


(b) Large horizon regime

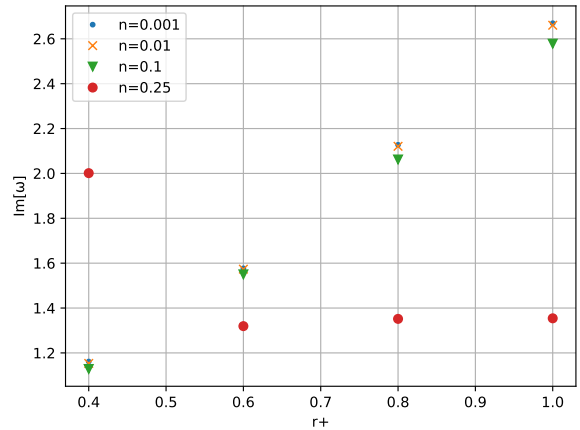
Figure 2: Lowest QNM regression wrt the black hole horizon.

Remarkably, when n approaches a critical value n_{cr} the lowest QNMs become overdamped as their real part drops abruptly towards zero. On the other hand, their imaginary part drops only slightly. This behaviour of ω_R, ω_I and $|\omega|$ is depicted in figures 3, 4.

The behaviour of the lowest QNM for values of the NUT charge close to and beyond the critical limit is shown in tables 3.



(a) Real part of the lowest QNM.



(b) Imaginary part of the lowest QNM.

Figure 3: Overdamping of the lowest QNM at the critical Nut charge limit for intermediate black holes.

Our numerical results show that the critical value n_{cr} where this overdamping takes place is almost the same for the whole range of r_+ that we considered. This begs an analytic explanation that we will now attempt. For a given r_+ and n we have introduced the bound $|\omega_*(r_+, n)|$ in (58) for

Table 3: The lowest QNMs of intermediate and large TNAdS₄ black holes for values of the NUT charge close to and beyond the critical value.

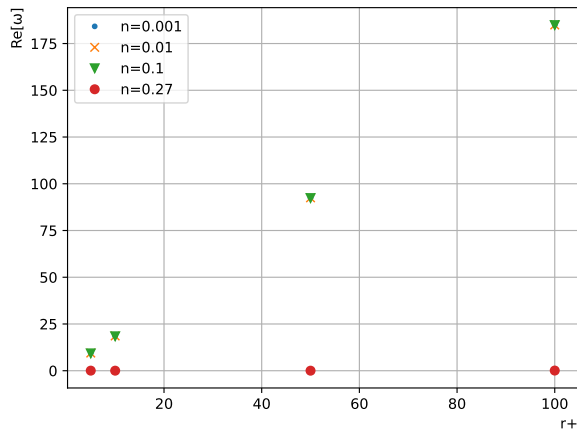
r_+	n	Re[ω]	-Im[ω]	$ \omega $
0.4	0.2	0.06	2.08	2.08
0.4	0.25	0.06	2	2
0.4	0.3	0.05	2.14	2.14
0.4	0.5	0.08	2.72	2.73
0.4	1	0.04	5.58	5.58
0.4	5	0.01	95.6	95.6
0.6	0.2	0.08	0.45	0.46
0.6	0.25	0.15	1.32	1.33
0.6	0.3	0.17	1.44	1.45
0.6	0.5	0.22	1.99	2
0.6	1	0.2	4.08	4.09
0.6	5	0.05	64.23	64.23
0.8	0.2	2.17	2.22	3.1
0.8	0.25	0.12	1.35	1.36
0.8	0.3	0.13	1.49	1.49
0.8	0.5	0.15	1.98	1.98
0.8	1	0.13	3.59	3.59
0.8	5	0.03	48.7	48.7
1	0.2	2.45	2.55	3.53
1	0.25	0.11	1.35	1.36
1	0.3	0.12	1.57	1.57
1	0.5	0.14	2.03	2.04
1	1	0.11	3.38	3.38
1	5	0.03	39.49	39.49

r_+	n	Re[ω]	-Im[ω]	$ \omega $
5	0.2	9.15	13.01	15.91
5	0.25	8.26	13.7	16
5	0.3	0.1	5.07	5.07
5	0.5	0.11	6.29	6.29
5	1	0.090	7.41	7.41
5	5	0.02	15.08	15.08
10	0.2	18.35	26.33	32.1
10	0.25	16.94	27.49	32.29
10	0.3	0.1	9.91	9.91
10	0.5	0.11	12.34	12.34
10	1	0.09	14.22	14.22
10	5	0.02	18.75	18.75
50	0.2	92.88	133	162.22
50	0.25	86.59	138.53	163.36
50	0.3	0.1	49.16	49.16
50	0.5	0.11	61.29	61.29
50	1	0.09	70.15	70.15
50	5	0.02	75.53	75.53
100	0.2	186.16	266.35	324.96
100	0.25	155.05	288.64	327.65
100	0.3	0.10	98.3	98.3
100	0.5	0.11	122.55	122.55
100	1	0.09	140.25	140.25
100	5	0.02	149.92	149.92

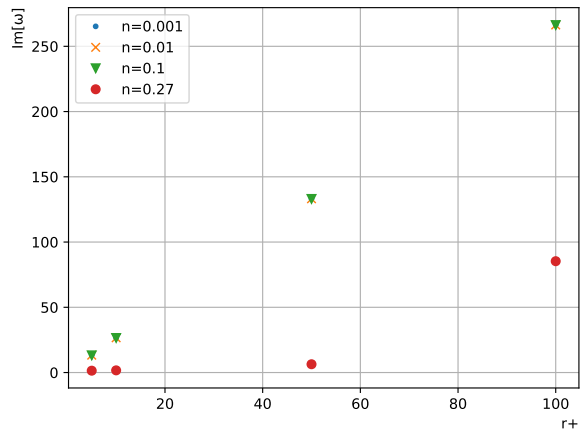
the stable QNM region. But according to our results the norm of the lowest stable QNM is related to r_+ for both the large and intermediate regimes as per the figures 2. The approximate relations for these regimes are shown in (73). Now as n increases, for a given r_+ , the bound $|\omega_*(r_+, n)|$ decreases and at some point it will become equal and then smaller than the norms (73). So equating the $|\omega_*(r_+, n)|$ with the norms (73) we will find the value n_{cr} beyond which the radius of the stable QNM region is smaller than the radius of the lowest QNM for a given r_+ . Assuming a generic behaviour $|\omega| = ar_+ + b$ we find

$$(ar_+ + b)^2 = \frac{1 + 3r_+^2 + 3n_{cr}^2}{4n_{cr}^2} \Rightarrow n_{cr} = \sqrt{\frac{1 + 3r_+^2}{4a^2r_+^2 + 4b^2 + 8abr_+ - 3}}. \quad (74)$$

Substituting then $a = 3.24, b = 0$ for large BHs, and $a = 2.07, b = 1, 74$ for intermediate BHs we can plot the rhs of (74) in figures 5 we see that for $r_+ \in [0.4, 100]$ we have $n_{cr} \in [0.25, 0.27]$. These are the values of the NUT charge for which we numerically observe the overdamping of the lowest stable QNMs. Clearly the above quantitative argument is not an analytic proof of our numerical results for the existence of n_{cr} . Nevertheless we believe that it shows the physical importance of



(a) Real part of the lowest QNM.



(b) Imaginary part of the lowest QNM.

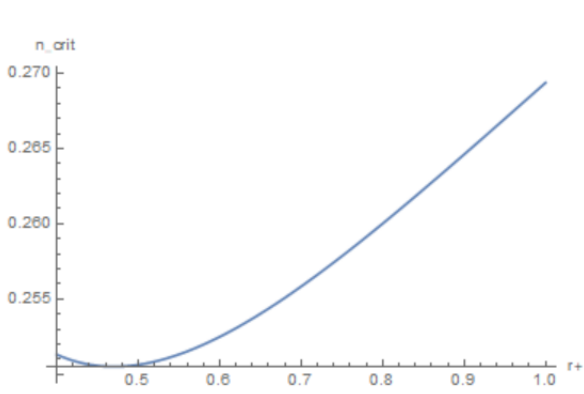
Figure 4: Overdamping of the lowest QNM at the critical Nut charge limit for large black holes.

the stable QNM region for the TNAdS₄ black holes.

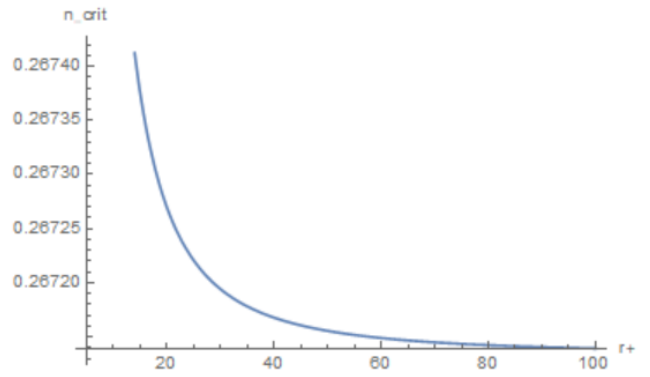
In figures 6 we plot the behaviour of the norm of the lowest mode for different values of the NUT charge in the large and intermediate BHs regimes. We notice that $|\omega|$ drops significantly for $n \approx n_{cr}$ but it starts increasing for larger values of n . The imaginary part of the lowest QNM increases sharply towards zero for values of NUT charge that approach the critical n . This is demonstrated in figures 7 for indicative values of the horizon. For larger values of the NUT charge it starts decreasing towards negative values.

We may further query how the NUT charge affect the higher overtones. For that we give in the following tables 4-7 the relevant results for the first ten overtones for the values $r_+ = 100, 1$ and various values of n up to n_{cr} . We notice that the presence of a non zero n has introduced a splitting of the two dual QNM modes as $[\omega, -\omega^*] \mapsto [(\omega_+, \omega_-), (-\omega_-^*, -\omega_+^*)]$ where we have denoted with ω_+ the mode with the larger positive real part. The difference $\Delta\omega = \omega_+ - \omega_-$ depends on n and appears to be maximum near n_{cr} . The study of this interesting property of the QNMs is beyond the scope of the present work, but we hope to return to this issue in the near future.

So far we have assumed $\mathcal{N} = 0$ in the definition (45) of the separation constant C of the angular equation. We can extend our analysis to non zero values of \mathcal{N} restricting ourselves to $\mathcal{N} \in [-2, 2]$. We study again the behaviour of the lowest QNM for various values of the NUT charge, using $r_+ = 1$ and $r_+ = 100$ as indicative horizon values for intermediate and large black holes respectively. The generic behaviour of the QNMs in the $\mathcal{N} = 0$ case still hold as it can be seen in table 8, where we notice a similar damping around the same critical values of the NUT charge for all cases. We also notice a slight asymmetry between positive and negative values of \mathcal{N} for which we do not have an explanation. Clearly this case deserves further investigation which is beyond the scope of the present work.



(a) Intermediate horizon regime.



(b) Large horizon regime.

Figure 5: Behaviour of the critical NUT charge for different horizons.

Table 4: The first 10 quasinormal modes for $r_+ = 1$, for various values of n .

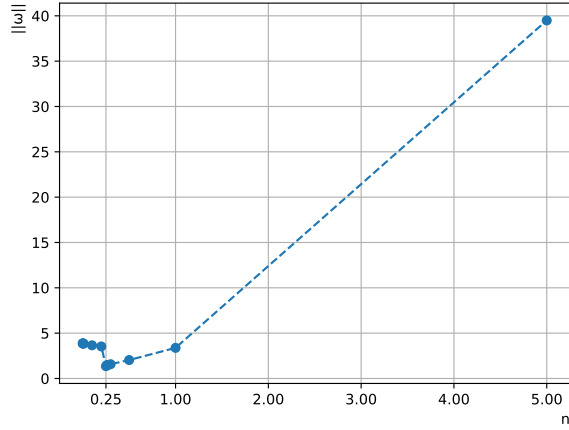
n	k	$\text{Re}[\omega]$	$\text{Im}[\omega]$
0	1	2.8	-2.67
0	2	-2.8	-2.67
0	3	4.77	-5.11
0	4	-4.77	-5.11
0	5	6.2	-6.91
0	6	-6.2	-6.91
0	7	9.81	-8.14
0	8	-9.81	-8.14
0	9	14.39	-11.3
0	10	-14.39	-11.3

n	k	$\text{Re}[\omega]$	$\text{Im}[\omega]$
0.01	1	2.78	-2.66
0.01	2	-2.82	-2.68
0.01	3	4.74	-5.09
0.01	4	-4.8	-5.12
0.01	5	6.17	-6.91
0.01	6	-6.23	-6.91
0.01	7	9.74	-8.13
0.01	8	-9.88	-8.14
0.01	9	14.29	-11.27
0.01	10	-14.5	-11.34

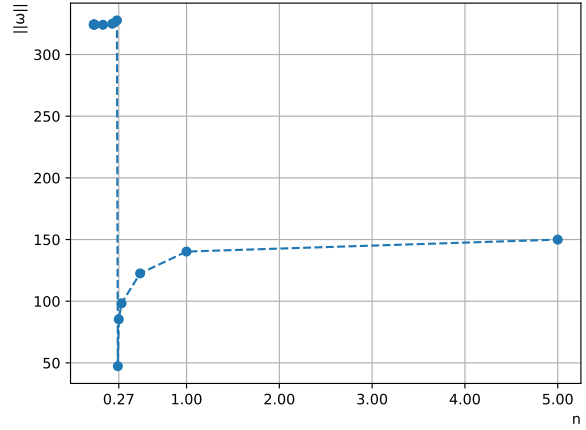
Table 5: The first 10 quasinormal modes for $r_+ = 1$, for various values of n .

n	k	$\text{Re}[\omega]$	$\text{Im}[\omega]$
0.1	1	2.6	-2.58
0.1	2	-3.07	-2.78
0.1	3	4.51	-4.96
0.1	4	-5.11	-5.34
0.1	5	5.96	-6.85
0.1	6	-6.62	-6.79
0.1	7	9.36	-8.1
0.1	8	-10.89	-8.21
0.1	9	13.78	-11.21
0.1	10	-16.02	-11.92

n	k	$\text{Re}[\omega]$	$\text{Im}[\omega]$
0.27	1	-0.11	-1.47
0.27	2	0.15	-4.18
0.27	3	-0.85	-5.07
0.27	4	2.	-6.85
0.27	5	-3.28	-7.53
0.27	6	4.11	-9.14
0.27	7	-6.12	-9.88
0.27	8	6.78	-11.73
0.27	9	-9.99	-12.93
0.27	10	9.85	-15.24

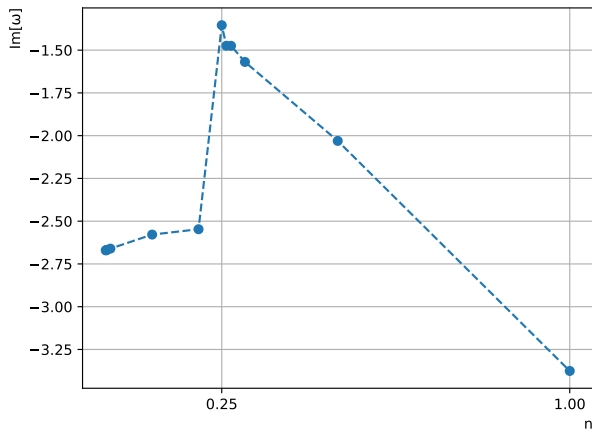


(a) $r_+ = 1$

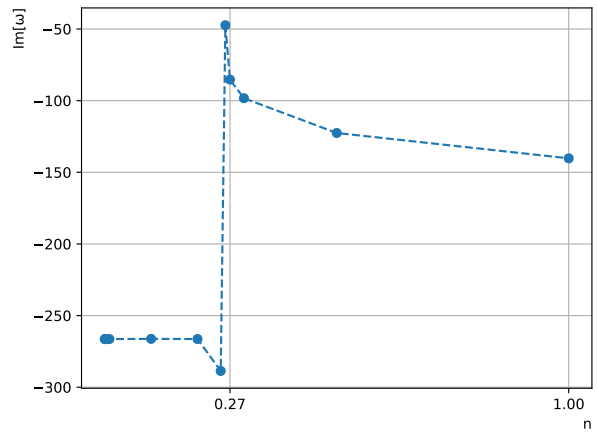


(b) $r_+ = 100$

Figure 6: $||\omega||$ of the lowest QNM for different values of the NUT charge.



(a) $r_+ = 1$



(b) $r_+ = 100$

Figure 7: Imaginary part of the lowest QNM for different values of the NUT charge close to the critical value.

Table 6: The first 10 quasinormal modes for $r_+ = 100$, for various values of n .

n	k	$\text{Re}[\omega]$	$\text{Im}[\omega]$	n	k	$\text{Re}[\omega]$	$\text{Im}[\omega]$
0	1	184.95	-266.39	0.01	1	184.93	-266.37
0	2	-184.95	-266.39	0.01	2	-184.98	-266.40
0	3	316.15	-491.64	0.01	3	316.12	-491.61
0	4	-316.15	-491.64	0.01	4	-316.18	-491.66
0	5	446.73	-717.16	0.01	5	446.70	-717.13
0	6	-446.73	-717.16	0.01	6	-446.77	-717.20
0	7	566.19	-943.82	0.01	7	566.15	-943.78
0	8	-566.19	-943.82	0.01	8	-566.21	-943.85
0	9	705.97	-1110.41	0.01	9	705.95	-1110.35
0	10	-705.97	-1110.41	0.01	10	-706.07	-1110.40

Table 7: The first 10 quasinormal modes for $r_+ = 100$, for various values of n .

n	k	$\text{Re}[\omega]$	$\text{Im}[\omega]$	n	k	$\text{Re}[\omega]$	$\text{Im}[\omega]$
0.1	1	184.84	-266.24	0.27	1	-0.09	-85.33
0.1	2	-185.28	-266.59	0.27	2	50.58	-336.78
0.1	3	316.45	-491.83	0.27	3	-51.54	-338.07
0.1	4	-317.02	-492.34	0.27	4	1.96	-560.62
0.1	5	448.28	-718.54	0.27	5	230.53	-586.13
0.1	6	-448.98	-719.15	0.27	6	-231.54	-585.77
0.1	7	568.38	-946.40	0.27	7	400.83	-771.17
0.1	8	-569.06	-946.99	0.27	8	-401.35	-771.17
0.1	9	719.78	-1108.06	0.27	9	545.37	-945.26
0.1	10	-720.90	-1108.30	0.27	10	-545.74	-945.35

Table 8: Lowest QNM against different values of the NUT charge for different values of \mathcal{N} , for indicative horizons.

r_+	\mathcal{N}	n	$\text{Re}[\omega]$	$-\text{Im}[\omega]$	$ \omega $	r_+	\mathcal{N}	n	$\text{Re}[\omega]$	$-\text{Im}[\omega]$	$ \omega $
1	-2.0	0.10	2.82	2.25	3.61	100	-2.0	0.10	184.42	265.88	323.58
1	-2.0	0.25	0.23	1.10	1.12	100	-2.0	0.27	0.280	85.32	85.32
1	-2.0	1	0.32	3.30	3.32	100	-2.0	1.00	0.27	140.25	140.25
1	-1.0	0.10	2.60	2.58	3.66	100	-1.0	0.10	184.84	266.24	324.11
1	-1.0	0.25	0.11	1.44	1.44	100	-1.0	0.27	0.09	85.33	85.33
1	-1.0	1	0.11	3.38	3.38	100	-1.0	1.00	0.09	140.25	140.25
1	1.0	0.10	2.82	2.25	3.61	100	1.0	0.10	184.42	265.88	323.58
1	1.0	0.25	0.23	1.10	1.12	100	1.0	0.27	0.28	85.32	85.32
1	1.0	1	0.32	3.30	3.32	100	1.0	1.00	0.27	140.25	140.25
1	2.0	0.10	3.41	2.01	3.96	100	2.0	0.10	184.01	265.51	323.04
1	2.0	0.25	0.18	0.54	0.57	100	2.0	0.27	0.47	85.31	85.31
1	2.0	1	0.50	3.17	3.21	100	2.0	1.00	0.45	140.25	140.25

5 Discussion

In this work we presented numerical results for the quasinormal modes of the massless scalar fluctuations in a Taub-NUT AdS₄ background. This work is a natural continuation of [15] where we have analytically studied the relevant fluctuation equations. The main issue identified in [15] was that the globally regular solutions of the angular equation are not compatible with the presence of complex quasinormal modes. In this work we ignored this issue and considered angular modes that correspond to highest weight $SU(2)$ representations, that are non-unitary and not globally regular. The resulting radial equation does not guarantee the stability of the QNMs. This is reminiscent of the case of odd gravitational fluctuations in Schwarzschild AdS₄ [6]. Nevertheless, we are able to show that there exists a region in QNM space that contains only stable modes. The radius of this stable QNM region increases with r_+ , thus larger BHs are more stable. For fixed r_+ the radius of the region shrinks as n increases, but curiously it reaches a constant non-zero value for infinite n .

The main result of our work is the existence of a critical NUT parameter n_{cr} such that for $n > n_{cr}$ the lowest QNMs are overdamped. Remarkably, the value of n_{cr} is rather insensitive to the horizon radius r_+ as we were able to argue semi-analytically. Moreover, we observed that the NUT charge induces a fine-splitting of the QNMs which becomes maximum near n_{cr} . These observations draw an interesting picture for the holographic fluid of TNAdS₄, in particular one in which n_{cr} separates an oscillating from an overdamped phase. We believe that this deserves further study.

An alternative holographic interpretation of Taub-NUT AdS₄ can be based on the regular solutions of the angular equation presented in the Appendix A. As we have mentioned, this picture corresponds to the quantization of Ω , hence there is no ringdown of the TNAdS₄ spacetime. We actually find that

$$2\Omega = 4n\omega = k, \quad k \in \mathbb{Z}^+. \quad (75)$$

This is the equivalent of the usual Dirac monopole quantization condition $2ge = k'$, $k' \in \mathbb{Z}^+$ if we identify $2n \leftrightarrow g$ and $\omega \leftrightarrow e$. From the fluid dynamics point of view this result corresponds to the quantization of the total circulation (11) as

$$C_{total}^{TN} = \left(\frac{2\pi\hbar}{M_{TN}} \right) k, \quad M_{TN} = \hbar\omega, \quad k \in \mathbb{Z}^+. \quad (76)$$

This coincides with the well-known condition for the circulation quantization of superfluid vortices, where M_{TN} is the mass of the condensate, see for example [37,38]. This result prompts us to suggest that the non-singular modes around the TNAdS₄ background can be interpreted as quantized vortices.

Acknowledgements

A.C.P. would like to acknowledge useful correspondence with M. Casals, R. Davison, B. Goutereaux, J. E. Santos, F. Willenborg, H. Zhang and the warm hospitality of CPHT \grave{E} cole Polytechnique and

A Regular solutions of the angular equation

The analysis of the $SU(2)$ irreps can be alternatively and equivalently performed by studying the angular differential equation (25). For example, for $\Omega = 0$ (26) is the associated Legendre equation whose solutions are the associated Legendre functions. Although the latter can be defined for generic complex values of ℓ and m [39], the quantization of these parameters arises by imposing the condition that the *physically acceptable* solutions are the Legendre polynomials which are regular over the whole range of the variable $u \in [0, 1]$ or equivalently $\theta \in [0, \pi]$. We will attempt a similar approach to our problem here and set $\Omega \neq 0$ from now on. Eq. (26) is a hypergeometric equation with solutions given by

$$Y_{\ell\mathcal{N}\Omega}(u) = \theta(\mathcal{N})C_1(1-u)^{\frac{\mathcal{N}+2\Omega}{2}}u^{\frac{\mathcal{N}}{2}}{}_2F_1(\mathcal{N}+\Omega-\ell, \mathcal{N}+\Omega+\ell+1, 1+\mathcal{N}; u) \\ + \theta(-\mathcal{N})C_2(1-u)^{\frac{\mathcal{N}+2\Omega}{2}}u^{-\frac{\mathcal{N}}{2}}{}_2F_1(\Omega-\ell, \Omega+\ell+1, 1-\mathcal{N}; u), \quad (77)$$

where C_1, C_2 are some generically complex constants. By using the theta functions in (77) we have ensured the regularity of the solution at $u = 0$ ($\theta = 0$) where it behaves as $Y(u) \xrightarrow{u \rightarrow 0} u^{|\mathcal{N}|/2}$. The regularity near $u = 1$ ($\theta = \pi$) must be separately considered and has physical consequences. We consider the cases $\mathcal{N} > 0$, $\mathcal{N} < 0$ and $\mathcal{N} = 0$ separately. For $\mathcal{N} > 0$ we have

$$Y_{\ell\mathcal{N}\Omega}(u) \xrightarrow{u \rightarrow 1} (1-u)^{\frac{1}{2}(\mathcal{N}+2\Omega)} \left(-\frac{\pi \csc[\pi(\mathcal{N}+2\Omega)]}{\Gamma(1+\mathcal{N}+2\Omega)} \frac{\Gamma(1+\mathcal{N})}{\Gamma(-\ell-\Omega)\Gamma(1+\ell-\Omega)} + \dots \right) + \\ + (1-u)^{-\frac{1}{2}(\mathcal{N}+2\Omega)} \left(\frac{(-1)^{-\mathcal{N}-2\Omega} \pi \csc[\pi(\mathcal{N}+2\Omega)]}{\Gamma(1-\mathcal{N}-2\Omega)} \frac{\Gamma(1+\mathcal{N})}{\Gamma(-\ell+\mathcal{N}+\Omega)\Gamma(1+\ell+\mathcal{N}+\Omega)} + \dots \right), \quad (78)$$

where the dot denote terms proportional to increasing powers of $1-u$. For a given $\ell > 0$ we must ensure that there is no singular term in (78). When $\mathcal{N}+2\Omega > 0$ the second line is singular¹¹ for $\mathcal{N}+\Omega = m = \ell - k$, $k = 0, 1, 2, 3, \dots$ with Ω and \mathcal{N} otherwise unrestricted. When $\mathcal{N}+2\Omega < 0$, the first line in (78) is singular and we must require that $\Omega = -\ell + n$, $n = 0, 1, 2, 3, \dots$ with \mathcal{N} unrestricted. On top of regularity, we want to require the single-valuedness of the eigenfunctions $Y_{\ell m \Omega}(\theta, \phi)$ under the rotation $\phi \rightarrow \phi + 2\pi n$, $n \in \mathbb{Z}$. This gives $m - \Omega = \mathcal{N} \in \mathbb{Z}$ which combined with the previous results yields $m - \Omega = 2\ell - k + n = \mathcal{N} \in \mathbb{Z}$. For generic integers k, n this implies that $\ell = M/2$, $M \in \mathbb{Z}$, namely we find that the $SU(2)$ eigenvalues are half-integers or integers when the corresponding eigenfunctions are regular and single-valued. Of course, when $\Omega = 0$ we return to the textbook result that requires ℓ to be integer for regular and single-valued eigenfunctions of the Laplacian on the two-sphere.

¹¹Notice that $\csc(\pi x)/\Gamma(1-x)$ is regular for $x = 1, 2, 3, \dots$

For $\Omega > m$ the solution near $u = 1$ behaves as

$$Y_{\ell\mathcal{N}\Omega}(u) \xrightarrow{u \rightarrow 1} (1-u)^{\frac{1}{2}(m+\Omega)} \left(-\frac{\pi \csc[\pi(m+\Omega)]}{\Gamma(1+m+\Omega)} \frac{\Gamma(1-m+\Omega)}{\Gamma(-m-\ell)\Gamma(1-m+\ell)} + \dots \right) + (1-u)^{-\frac{1}{2}(m+\Omega)} \left(\frac{\pi \csc[(-1)^{-m-\Omega}\pi(m+\Omega)]}{\Gamma(1-m-\Omega)} \frac{\Gamma(1-m+\Omega)}{\Gamma(-\ell+\Omega)\Gamma(1+\ell+\Omega)} + \dots \right). \quad (79)$$

This is obtained from (78) under the map $m \leftrightarrow \Omega$ which implies that our analysis will yield m and Ω to be integers *or* half-integers satisfying $-\ell \leq m < \Omega \leq \ell$, depending on whether $\ell > 0$ is correspondingly an integer or a half-integer.

For $\Omega = m$ there is no ϕ dependence in (24), nevertheless there is still a non-trivial "magnetic" quantum number since the solution becomes

$$Y_{\ell\mathcal{N}\Omega}(u) \xrightarrow{\mathcal{N} \rightarrow 0} C(1-u)^m {}_2F_1(-\ell+m, 1+\ell+m; 1, u). \quad (80)$$

Requiring this to be regular at $u = 0, 1$ we obtain again that m is an integer *or* a half-integer with $|m| \leq \ell$.

To summarize, we have found regular solutions of the angular equation (25) which are single valued as $\phi \mapsto \phi + 2n\pi$, $n \in \mathbb{Z}$, under the requirement that m and Ω are integers *or* half-integers satisfying $-\ell \leq m, \Omega \leq \ell$, with $\ell = 0, 1/2, 1, 3/2, 2, \dots$. Explicitly, the general solution of the scalar fluctuation equation (13) is given by

$$\Phi(t, r, \theta, \phi) = e^{-i\omega t} e^{i\mathcal{N}\phi} Y_{\ell\mathcal{N}\Omega}(\theta) R(r), \quad \mathcal{N} = m - \Omega \in \mathbb{Z}. \quad (81)$$

Notice now that due to (75) the solution (81) is periodic in the time coordinate under shifts of the form

$$t \rightarrow t + 8\pi nk, \quad k \in \mathbb{Z}. \quad (82)$$

This is exactly the usual Misner-string periodicity condition [20, 22], and we are describing a smooth $U(1)$ bundle.

References

- [1] V. E. Hubeny, S. Minwalla, and M. Rangamani, "The fluid/gravity correspondence," in *Theoretical Advanced Study Institute in Elementary Particle Physics: String theory and its Applications: From meV to the Planck Scale*, pp. 348–383, 2012.
- [2] E. Berti, V. Cardoso, and A. O. Starinets, "Quasinormal modes of black holes and black branes," *Class. Quant. Grav.*, vol. 26, p. 163001, 2009.
- [3] R. A. Konoplya and A. Zhidenko, "Quasinormal modes of black holes: From astrophysics to string theory," *Rev. Mod. Phys.*, vol. 83, pp. 793–836, 2011.

- [4] S. A. Hartnoll, A. Lucas, and S. Sachdev, “Holographic quantum matter,” 12 2016.
- [5] G. T. Horowitz and V. E. Hubeny, “Quasinormal modes of AdS black holes and the approach to thermal equilibrium,” *Phys. Rev. D*, vol. 62, p. 024027, 2000.
- [6] V. Cardoso and J. P. S. Lemos, “Quasinormal modes of Schwarzschild anti-de Sitter black holes: Electromagnetic and gravitational perturbations,” *Phys. Rev. D*, vol. 64, p. 084017, 2001.
- [7] V. Cardoso, R. Konoplya, and J. P. S. Lemos, “Quasinormal frequencies of Schwarzschild black holes in anti-de Sitter space-times: A Complete study on the asymptotic behavior,” *Phys. Rev. D*, vol. 68, p. 044024, 2003.
- [8] G. Michalogiorgakis and S. S. Pufu, “Low-lying gravitational modes in the scalar sector of the global AdS(4) black hole,” *JHEP*, vol. 02, p. 023, 2007.
- [9] V. Cardoso, O. J. C. Dias, G. S. Hartnett, L. Lehner, and J. E. Santos, “Holographic thermalization, quasinormal modes and superradiance in Kerr-AdS,” *JHEP*, vol. 04, p. 183, 2014.
- [10] N. Uchikata, S. Yoshida, and T. Futamase, “Scalar perturbations of Kerr-AdS black holes,” *Phys. Rev. D*, vol. 80, p. 084020, 2009.
- [11] B. Wang, C.-Y. Lin, and E. Abdalla, “Quasinormal modes of Reissner-Nordstrom anti-de Sitter black holes,” *Phys. Lett. B*, vol. 481, pp. 79–88, 2000.
- [12] B. Wang, C. Molina, and E. Abdalla, “Evolving of a massless scalar field in Reissner-Nordstrom Anti-de Sitter space-times,” *Phys. Rev. D*, vol. 63, p. 084001, 2001.
- [13] E. Berti and K. D. Kokkotas, “Quasinormal modes of Reissner-Nordström-anti-de Sitter black holes: Scalar, electromagnetic and gravitational perturbations,” *Phys. Rev. D*, vol. 67, p. 064020, 2003.
- [14] F. Ficek and C. Warnick, “Quasinormal modes of Reissner–Nordström–AdS: the approach to extremality,” *Class. Quant. Grav.*, vol. 41, no. 8, p. 085011, 2024.
- [15] G. Kalamakis, R. G. Leigh, and A. C. Petkou, “Aspects of holography of Taub-NUT- AdS₄ spacetimes,” *Phys. Rev. D*, vol. 103, no. 12, p. 126012, 2021.
- [16] P. A. Cano and D. Pereñiguez, “Quasinormal modes of NUT-charged black branes in the AdS/CFT correspondence,” *Class. Quant. Grav.*, vol. 39, no. 16, p. 165003, 2022.
- [17] A. Al-Badawi, S. Kanzi, and I. Sakalli, “Greybody radiation of scalar and Dirac perturbations of NUT black holes,” *Eur. Phys. J. Plus*, vol. 137, no. 1, p. 94, 2022.

- [18] G. Clément, D. Gal'tsov, and M. Guenouche, “Rehabilitating space-times with NUTs,” *Phys. Lett. B*, vol. 750, pp. 591–594, 2015.
- [19] R. A. Hennigar, D. Kubiznak, and R. B. Mann, “Thermodynamics of Lorentzian Taub-NUT spacetimes,” 2019.
- [20] C. W. Misner, “The Flatter regions of Newman, Unti and Tamburino’s generalized Schwarzschild space,” *J. Math. Phys.*, vol. 4, pp. 924–938, 1963.
- [21] W. B. Bonnor, “A new interpretation of the NUT metric in general relativity,” *Math. Proc. Cambridge Phil. Soc.*, vol. 66, no. 1, pp. 145–151, 1969.
- [22] D. Astefanesei, R. B. Mann, and E. Radu, “Nut charged space-times and closed timelike curves on the boundary,” *JHEP*, vol. 01, p. 049, 2005.
- [23] T. T. Wu and C. N. Yang, “Dirac Monopole Without Strings: Monopole Harmonics,” *Nucl. Phys.*, vol. B107, p. 365, 1976.
- [24] T. Dray, “The Relationship Between Monopole Harmonics and Spin Weighted Spherical Harmonics,” *J. Math. Phys.*, vol. 26, p. 1030, 1985.
- [25] M. Casals, A. C. Ottewill, and N. Warburton, “High-order asymptotics for the Spin-Weighted Spheroidal Equation at large real frequency,” *Proc. Roy. Soc. Lond. A*, vol. 475, no. 2222, p. 20180701, 2019.
- [26] F. Willenborg, D. Philipp, and C. Lämmerzahl, “The scalar angular Teukolsky equation and its solution for the Taub-NUT spacetime,” 11 2024.
- [27] O. J. C. Dias and J. E. Santos, “Boundary Conditions for Kerr-AdS Perturbations,” *JHEP*, vol. 10, p. 156, 2013.
- [28] M. Blake and R. A. Davison, “Chaos and pole-skipping in rotating black holes,” *JHEP*, vol. 01, p. 013, 2022.
- [29] X.-h. Chu, Y.-q. Chu, S.-s. Bao, and H. Zhang, “Next-to-leading order corrections to scalar perturbations of Kerr-anti-de Sitter black holes,” *Phys. Rev. D*, vol. 111, no. 4, p. 043039, 2025.
- [30] R. G. Leigh, A. C. Petkou, and P. M. Petropoulos, “Holographic Three-Dimensional Fluids with Nontrivial Vorticity,” *Phys. Rev.*, vol. D85, p. 086010, 2012.
- [31] R. G. Leigh, A. C. Petkou, and P. M. Petropoulos, “Holographic Fluids with Vorticity and Analogue Gravity,” *JHEP*, vol. 11, p. 121, 2012.

- [32] A. Mukhopadhyay, A. C. Petkou, P. M. Petropoulos, V. Pozzoli, and K. Siampos, “Holographic perfect fluidity, Cotton energy-momentum duality and transport properties,” *JHEP*, vol. 04, p. 136, 2014.
- [33] E. Berti, V. Cardoso, and M. Casals, “Eigenvalues and eigenfunctions of spin-weighted spheroidal harmonics in four and higher dimensions,” *Phys. Rev. D*, vol. 73, p. 024013, 2006. [Erratum: *Phys.Rev.D* 73, 109902 (2006)].
- [34] A. G. Shah and B. F. Whiting, “Raising and Lowering operators of spin-weighted spheroidal harmonics,” *Gen. Rel. Grav.*, vol. 48, no. 6, p. 78, 2016.
- [35] Y. M. Shnir, *Magnetic Monopoles*. Text and Monographs in Physics, Berlin/Heidelberg: Springer, 2005.
- [36] N. Drukker, B. Fiol, and J. Simon, “Godel type universes and the Landau problem,” *JCAP*, vol. 10, p. 012, 2004.
- [37] A. L. Fetter, “Rotating trapped Bose-Einstein condensates,” *Rev. Mod. Phys.*, vol. 81, pp. 647–691, 2009.
- [38] L. Pitaevskii and S. Stringari, *Bose-Einstein condensation and superfluidity*. Oxford University Press, 2016.
- [39] R. S. Maier, “Associated legendre functions and spherical harmonics of fractional degree and order,” *Constr Approx*, vol. 48, no. arXiv:1702.08555, pp. 235–281, 2018.